

## ORIGINAL ARTICLE

# Spatial proteomic profiling of tumor and stromal compartments in non-small-cell lung cancer identifies signatures associated with overall survival

Vahid Yaghoubi Naei<sup>1,2</sup>, James Monkman<sup>2</sup>, Habib Sadeghirad<sup>2</sup>, Ahmed Mehdi<sup>3</sup>, Tony Blick<sup>2</sup>, William Mullally<sup>4</sup>, Ken O'Byrne<sup>4</sup>, Majid Ebrahimi Warkiani<sup>1</sup> & Arutha Kulasinghe<sup>2</sup>  <sup>1</sup>School of Biomedical Engineering, University of Technology Sydney, Sydney, NSW, Australia<sup>2</sup>Frazer Institute, Faculty of Medicine, The University of Queensland, Brisbane, QLD, Australia<sup>3</sup>Queensland Cyber Infrastructure Foundation (QCIF) Ltd, The University of Queensland, Brisbane, QLD, Australia<sup>4</sup>The Princess Alexandra Hospital, Brisbane, QLD, Australia**Correspondence**A Kulasinghe, Frazer Institute, Faculty of Medicine, The University of Queensland, 37 Kent Street, Woolloongabba, QLD 4102, Australia.  
E-mail: [arutha.kulasinghe@uq.edu.au](mailto:arutha.kulasinghe@uq.edu.au)

Received 27 May 2024;

Revised 4 July 2024;

Accepted 5 July 2024

doi: 10.1002/cti2.1522

*Clinical & Translational Immunology*

2024; 13: e1522

**Abstract**

**Objectives.** Non-small-cell lung carcinoma (NSCLC) is the most prevalent and lethal form of lung cancer. The need for biomarker-informed stratification of targeted therapies has underpinned the need to uncover the underlying properties of the tumor microenvironment (TME) through high-plex quantitative assays. **Methods.** In this study, we profiled resected NSCLC tissues from 102 patients by targeted spatial proteomics of 78 proteins across tumor, immune activation, immune cell typing, immunology, drug targets, cell death and PI3K/AKT modules to identify the tumor and stromal signatures associated with overall survival (OS). **Results.** Survival analysis revealed that stromal CD56 (HR = 0.384,  $P = 0.06$ ) and tumoral TIM3 (HR = 0.703,  $P = 0.05$ ) were associated with better survival in univariate Cox models. In contrast, after adjusting for stage, BCLXL (HR = 2.093,  $P = 0.02$ ) and cleaved caspase 9 (HR = 1.575,  $P = 0.1$ ) negatively influenced survival. Delta testing indicated the protective effect of TIM-3 (HR = 0.614,  $P = 0.04$ ) on OS. In multivariate analysis, CD56 (HR = 0.172,  $P = 0.001$ ) was associated with better survival in the stroma, while B7.H3 (HR = 1.72,  $P = 0.008$ ) was linked to poorer survival in the tumor. **Conclusions.** Deciphering the TME using high-plex spatially resolved methods is giving us new insights into compartmentalised tumor and stromal protein signatures associated with clinical endpoints in NSCLC.

**Keywords:** digital spatial profiling, non-small-cell lung cancer, spatial proteomics, tumor microenvironment

**INTRODUCTION**

Non-small-cell lung cancer (NSCLC) and small-cell lung cancer (SCLC) are the most diagnosed and

deadliest subtypes of lung cancer worldwide.<sup>1–3</sup> Approximately 80% of lung cancer cases are caused by smoking exposure to carcinogens, in addition to rare genetic predispositions.<sup>4,5</sup>

Surgery, radiation therapy, chemotherapy and, more recently, targeted therapy and immunotherapy are treatment options for lung cancer.<sup>6,7</sup> Immunotherapy, alone or combined with chemotherapy, is the current regimen for patients without actionable mutations and has led to improved progression-free survival (PFS) and overall survival (OS).<sup>8,9</sup>

There is mounting evidence that the study of the tumor microenvironment (TME) is crucial for understanding tumor characteristics and the effectiveness of treatments.<sup>10–12</sup> The TME comprises complex mixtures of soluble chemokines in the extracellular matrix, fibroblasts, endothelial cells and innate and adaptive immune cells, into which tumor cells must invade and evade to proliferate.<sup>13</sup> The cellular interactions with nearby cells in this milieu drive dynamic phenotypic expression of cellular markers in both tumor and non-tumor cells.<sup>14</sup> Thus, studying the variations in marker expression provides a unique insight into the complex network of cell–cell interactions in the tumor microenvironment.<sup>15,16</sup> This reveals not only important indicators of interactions but also may uncover molecular mediators that influence the TME to favor tumor growth.<sup>17</sup> Over the past few years, the TME of NSCLC has emerged as an essential driver in the progression of primary lung cancer cases, responsible for its aggressiveness and resistance to anticancer therapies.<sup>18,19</sup>

Digital spatial profiling (DSP) maps biomolecules at a regional resolution within the spatial context of tissue morphology, allowing for a more complete understanding of the spatial relationships of tumor and non-tumor regions and potentially influencing tumorigenesis.<sup>20,21</sup> High multiplexing additionally enables the simultaneous study of numerous biomarkers within their tissue architecture with high detection sensitivity and specificity.<sup>22</sup> This technique enables biomarker identification and subsequent insights into the tumor microenvironment, resulting in increased depth for the discovery of novel therapeutic targets.<sup>23,24</sup>

## RESULTS

### NSCLC patient cohort

Our cohort consists of early (Stages I and II) and advanced (Stages III and IV) patient samples constructed across two TMAs. The cohort was

**Table 1.** Clinicopathological information about patients

	Cohort 1 (N = 37)	Cohort 2 (N = 65)	Overall (N = 102)
Gender			
Male	27 (73%)	40 (61.5%)	67 (65.7%)
Female	10 (27%)	25 (38.5%)	35 (34.3%)
Age			
Median	68 (46,83)	72 (41,86)	70 (41,86)
Stage			
IA	4 (10.8%)	15 (23.1%)	19 (18.6%)
IB	13 (35.2%)	19 (29.2%)	32 (31.4%)
IIA	1 (2.7%)	5 (7.7%)	6 (5.9%)
IB-IIA	0 (0%)	7 (10.8%)	7 (6.9%)
IIB	7 (18.9%)	14 (21.5%)	21 (20.6%)
IIIA	7 (18.9%)	3 (4.6%)	10 (9.8%)
IIIB	1 (2.7%)	2 (3.1%)	3 (2.9%)
IV	4 (10.8%)	0 (0%)	4 (3.9%)
Subtype			
Adenocarcinoma (ADC)	21 (56.7%)	54 (83%)	75 (73.5%)
Squamous cell carcinoma (SCC)	26 (70.2%)	0	26 (25.4%)
Unclassified	1 (2.7%)	0 (0%)	1 (0.9%)
Mutation			
KRAS			
Wild type	5 (13.5%)	0 (0%)	5 (4.9%)
Mutant	1 (2.7%)	0 (0%)	1 (0.9%)
Unknown	31 (83.7%)	65 (100%)	96 (94.1%)
EGFR			
Wild type	5 (13.5%)	0 (0%)	5 (4.9%)
Mutant	0 (0%)	0 (0%)	0 (0%)
Unknown	32 (86.4%)	65 (100%)	97 (95.1%)
Survival status			
Alive	24 (64.9%)	35 (53.8%)	59 (57.8%)
Deceased	13 (35.1%)	30 (46.2%)	43 (42.2%)

composed of 65.7% male and 34.3% female (Table 1). TMA cores were collected at resection, and survival status was calculated from the time of surgery to the final follow-up.

### Identification of differentially expressed proteins by the Nanostring GeoMx DSP assay

Using Nanostring GeoMx<sup>®</sup> DSP technology, multiplex proteomics of 102 TMA cores was performed (Figure 1). Regions were segmented into tumor (PanCK<sup>+</sup>) and stroma (PanCK<sup>-</sup>) to determine protein expression within tissue compartments. To inspect the integrity of our data, we first performed differential expression between tumor and stroma compartments (Figure 2b–e). In stroma regions, cell death markers, immune regulatory markers and myeloid markers were more common, while tumor areas

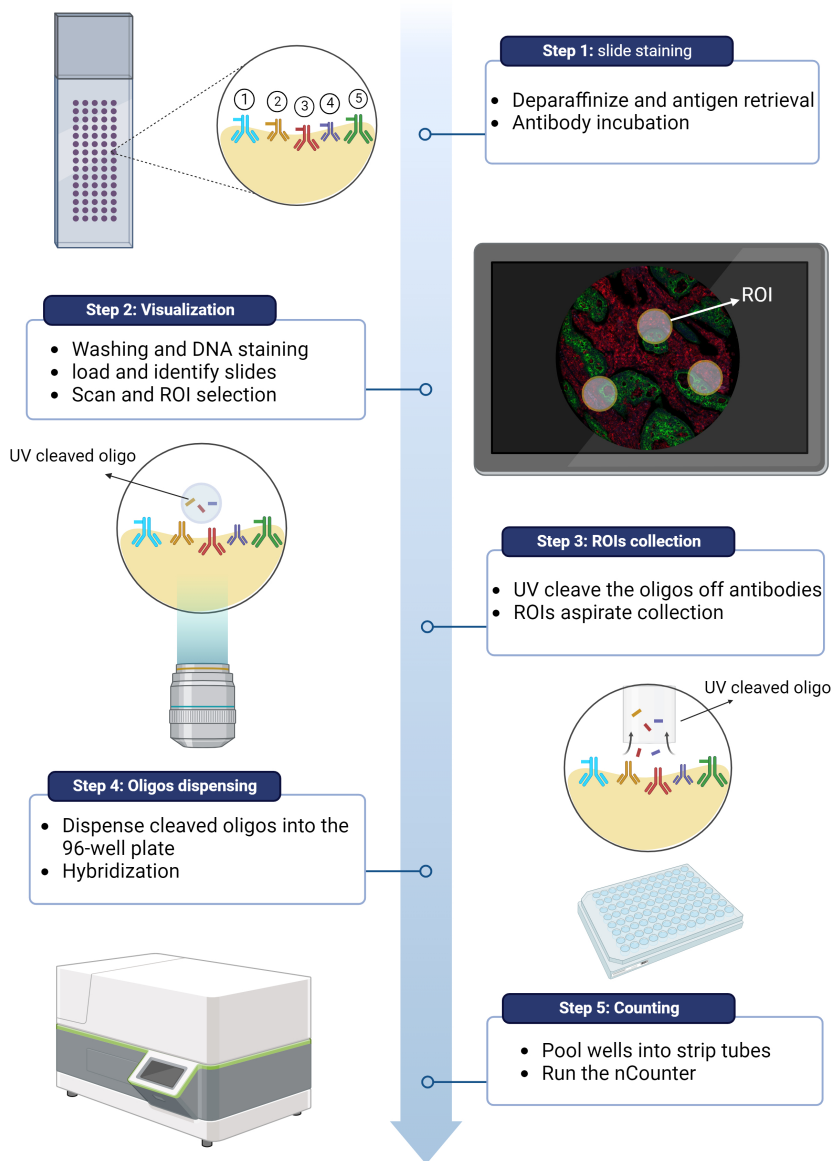


**Figure 1.** Overview of the digital spatial profiling workflow. In the first step, conjugated antibodies with DNA oligos bind to the target antigens. Through the visualising markers, region of interests (ROIs) are selected and UV-cleaved oligos are collected into specific wells and counted. The figure was generated by Biorender.

were enriched with immune-modulating and immune-activating markers. B-cell lymphoma extra large (BCLXL), P53, BCL2 antagonist of cell death (BAD), CD127, poly ADP-ribose polymerase (PARP), cleaved caspase 9, B-cell lymphoma 6 (BCL6), Bcl-2-like protein 11 (BIM), forkhead box protein P3 (FOXP3), PD-L2 and CD25 are the most upregulated markers in tumor compartments, whereas the expression of smooth muscle actin (SMA), fibronectin, CD3, CD4, CD45, CD163, CD34,

CD14 and CD68 decreased (Figure 2d and e) (Supplementary table 1).

### Univariate survival analysis

A Cox proportional hazards model and Kaplan–Meier (KM) survival model were applied to each protein to determine the association between protein expression and OS. In the continuous Cox model for the stromal compartment, CD56, a



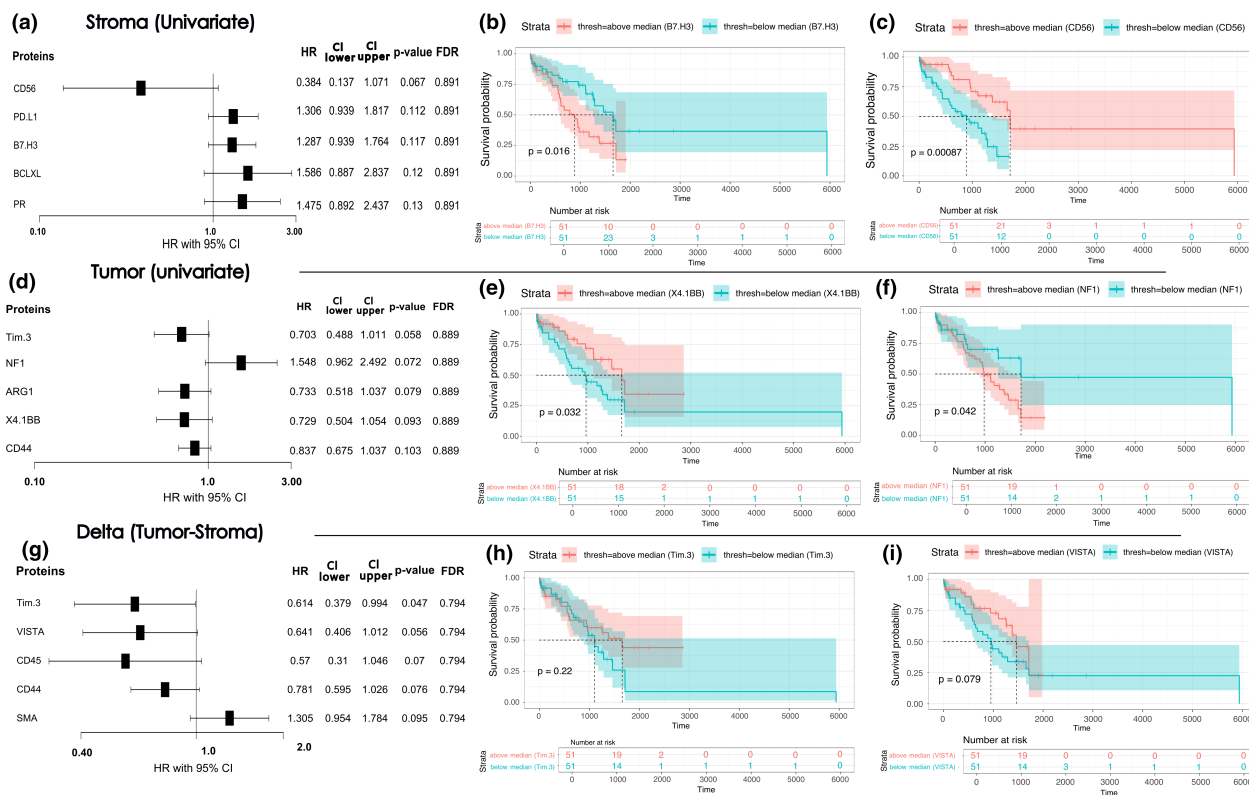


**Figure 3.** Analysis of overall survival (OS)-associated proteins. **(a)** Univariate CoxPH forest plot indicating hazard ratio with 95% confidence interval for proteins from the stroma regions. **(b, c)** Kaplan–Meier plots of stromal CD56 and B7-H3. **(d)** Univariate CoxPH forest plot indicating hazard ratio with 95% confidence interval for proteins from tumor regions. **(e, f)** Kaplan–Meier plots of tumoral 4.1BB and NF1. **(g)** CoxPH models for delta protein expression (tumor–stroma). **(h, i)** Kaplan–Meier plots of delta protein expression for TIM-3 and VISTA. HR >1 demonstrates an association with poorer OS. Threshold above median = red. Threshold below median = green.

marker of natural killer (NK) cells, showed a positive association with survival (HR = 0.384,  $P = 0.067$ ), approaching statistical significance, with KM analysis confirming this protective effect ( $P = 0.00087$ ) (Figure 3a and c). Conversely, immune checkpoint molecules B7-H3 (HR = 1.287,  $P = 0.1$ ) and PDL1 (HR = 1.306,  $P = 0.11$ ) along with the anti-apoptotic marker BCLXL (HR = 1.586,  $P = 0.1$ ) were linked to poorer survival outcomes. Kaplan–Meier estimates for PDL1 ( $P = 0.06$ ), B7-H3 ( $P = 0.01$ ) and BCLXL ( $P = 0.1$ ) supported Cox results associated with adverse survival prognosis (Figure 3a and b).

Cox regression of markers within the tumor regions indicated the tumor suppressor neurofibromin 1 (NF1) (HR = 1.548,  $P = 0.072$ ) associated with poorer survival. Conversely, higher expression of other markers was linked with improved survival outcomes. TIM3 (HR = 0.703,  $P = 0.05$ ), an immune checkpoint receptor, positively impacted survival. Similarly, arginase 1

(ARG1), which negatively affects T cell function (HR = 0.733,  $P = 0.07$ ), and CD44, known for its association with cancer stem cell properties (HR = 0.837,  $P = 0.1$ ), were linked to better survival rates. In addition, T cell activation marker 4.1BB (HR = 0.729,  $P = 0.09$ ) also indicated more favorable survival outcomes in Cox models (Figure 3d). Survival analysis by Kaplan–Meier suggested that only higher expression of ARG1 ( $P = 0.05$ ) was associated with better survival, while TIM3 ( $P = 0.3$ ), NF1 ( $P = 0.04$ ) (Figure 3f), 4.1BB ( $P = 0.03$ ) (Figure 3e) and CD44 ( $P = 0.5$ ) were linked to diminished survival.

The ‘Delta test’ is a method for determining the difference in relative expression levels of a marker in tumor regions compared to the stroma, generally represented as  $\delta$  ( $\delta = \text{Expression tumor} - \text{Expression stroma}$ ). This approach is beneficial in identifying the relative enrichment of markers that may have a greater impact within the tumor bulk, such as markers of immune cell function.

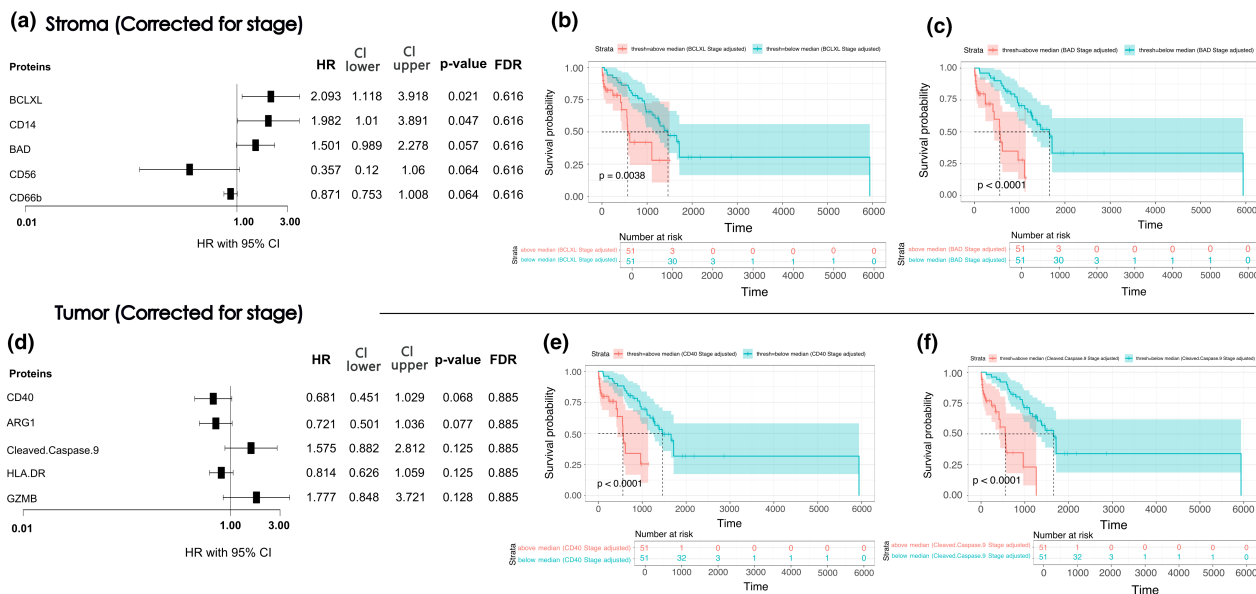


**Figure 4.** Analysis of overall survival (OS)-associated proteins corrected for stage. **(a)** CoxPH model for stromal protein expression corrected for stage. **(b, c)** Kaplan–Meier survival curves for stromal BCLXL and BAD expression corrected for stage. **(d)** CoxPH model for tumoral protein expression corrected for stage. **(e, f)** Kaplan–Meier survival curves for stromal CD40 and cleaved caspase 9 expression corrected for stage. HR >1 demonstrates an association with poorer OS. Threshold above median = red. Threshold below median = green.

Indeed, the Delta test indicated protective CoxPH trends for TIM-3, VISTA, CD45 and CD44. TIM-3 (HR = 0.614,  $P = 0.04$ ) and VISTA (HR = 0.641,  $P = 0.05$ ) were immune checkpoint molecules associated with a reduced risk of mortality in continuous Cox models. Similar positive survival associations were observed for T cell activation, signalling and migration markers such as CD45 (HR = 0.57,  $P = 0.07$ ) and CD44 (HR = 0.781,  $P = 0.07$ ) (Figure 3g). Conversely, higher expression of SMA (HR = 1.305,  $P = 0.09$ ) in the Delta test indicated reduced survival time in both Cox and KM survival estimates results.

**Univariates corrected for stage**

To examine the independent effects of each marker while adjusting the potential influence of patient effects, we corrected the survival results for the disease stage. After correcting for stage in stromal regions, upregulated anti-apoptotic markers BCLXL (HR = 2.093,  $P = 0.02$ ) and BAD (HR = 1.982,  $P = 0.04$ ) were found to correspond with worse survival outcomes. CD14 (HR = 1.501,  $P = 0.05$ ), a marker of M2 macrophage polarisation and immune suppression, was also associated with poorer outcomes (Figure 4a). In line with Cox models, KM survival analysis of

BCLXL ( $P = 0.0038$ ) (Figure 4b), BAD ( $P < 0.0001$ ) (Figure 4c) and CD14 ( $P < 0.0001$ ) provided similar survival outcomes, contrary to CD56 ( $P < 0.0001$ ) and CD66b ( $P < 0.0001$ ) showed different trends compared to Cox model.

In tumor regions, continuous survival regression analysis for antigen-presenting cell (APCs) markers CD40 (HR = 0.681,  $P = 0.06$ ) (Figure 4d and e) and HLA DR (HR = 0.814,  $P = 0.1$ ) in addition to ARG1 (HR = 0.721,  $P = 0.07$ ) was indicative of prolonged survival time (Figure 4d). We found apoptosis mediator-cleaved caspase 9 (HR = 1.575,  $P = 0.1$ ) (Figure 4f) and GZMB (HR = 1.777,  $P = 0.1$ ), which enhance antitumor immunity to be linked with poorer survival in both analyses.

**Multivariate model after variable selection using stepwise Cox regression analyses**

Multivariate analysis is a statistical approach for evaluating the impact of several variables on survival outcomes at once, allowing for the adjustment of confounding factors and the identification of independent survival predictors. This technique is instrumental in survival analysis for determining how numerous factors combine to determine survival rates.

**Table 2.** Multivariate model after variable selection using the CoxPH model

	exp (coef)	se (coef)	z	Pr (> z )
Multivariate model after variable selection using stepwise Cox regression analyses for stroma				
CD56	0.172	0.559	−3.151	0.00163
B7.H3	1.72	0.205	2.65	0.00805
CD20	2.32	0.372	2.262	0.0237
LAG3	2.009	0.271	2.578	0.00993
PDL1	1.418	0.159	2.192	0.0284
Multivariate model after variable selection using stepwise Cox regression analyses for tumor				
TIM-3	0.733	0.189	−1.642	0.1005
ARG1	0.694	0.164	−2.231	0.0257
NF1	1.601	0.269	1.75	0.08019
Multivariate model after variable selection using stepwise Cox regression analyses for delta expression (tumor-stroma)				
SMA	2.232	0.235	3.413	0.00064
4.1BB	0.648	0.185	−2.347	0.01893
Fibronectin	0.58	0.21	−2.596	0.00943
CD44	0.668	0.165	−2.443	0.01457

Multivariate analysis of our study reports stromal CD56 associated with improved survival outcomes while upregulated B7.H3, CD20, LAG3 and PDL1 reduced survival rate. A multivariate model after variable selection using stepwise Cox regression analyses for delta expression (Tumor–Stroma) revealed a significant association between SMA and worse survival opposite to 4.1BB, fibronectin and CD44 (Table 2).

## DISCUSSION

Non-small-cell lung cancer continues to be the leading cause of cancer-related deaths globally, posing a significant therapeutic obstacle.<sup>25–27</sup> Most patients are diagnosed with advanced stages of their condition, rendering surgical interventions no longer feasible. This emphasises the immediate demand for improved therapeutic methods, namely in targeted therapy, to control and potentially reverse the advancement of the disease.<sup>28</sup> In contrast to the significant improvements made by targeted and immunotherapy in advanced-stage disease, chemotherapy remains the essential choice for resected patients with stage II–IIIa disease with a 5-year survival benefit of 5%.<sup>29</sup> A variety of factors can cause chemotherapy failures in NSCLC patients, including tumor heterogeneity and acquired drug resistance.<sup>30,31</sup>

Integrating multiplexed molecular assays with spatial context can deeply aid our understanding of tumor heterogeneity, shed light on treatment resistance mechanisms and provide direction for novel treatment approaches.<sup>32,33</sup> This study assessed the inter- and intratumor differences in protein

expression of NSCLC tissue samples to investigate biomarkers indicative of patient outcome. We found that a diverse array of biomarkers, including cell adhesion molecules, immunological regulators, immune checkpoint inhibitors and apoptotic markers, are associated with survival outcomes in NSCLC patients. Anti-apoptotic proteins like BCLXL are released from the cells to prevent cell death. There are, however, some pro-apoptotic proteins, such as BAD, that counteract this by acting as antagonists to synergise with other apoptotic proteins, including cleaved caspase 9, to activate the intrinsic apoptosis pathway.<sup>34–36</sup> Surprisingly, it has been shown that caspase 9 enhances NSCLC tumorigenicity and correlates with an anti-apoptotic phenotype.<sup>37–39</sup> Our findings show that BCLXL, BAD and cleaved caspase 9 have a notable connection to survival outcomes, particularly after adjusting for the disease stage. All three mentioned markers were strongly linked to shorter survival, implying that their overexpression may enhance tumor resistance to apoptosis. CD56 is documented to be expressed mostly on NK cells in several cancers like lung and renal cell carcinoma.<sup>40–44</sup> CD56<sup>+</sup> NK cell enrichment level in the stroma was found to be favorably correlated to a higher survival index.<sup>45–47</sup> CD56 has consistently shown a protective effect on survival in the current study, highlighting its function in the immune response. A study showed its adverse effect upon correcting the stromal expression for stage. This may be caused by the advanced stage of cancer dominating the protective capabilities of immune cells.<sup>48,49</sup> Besides CD56, the integral role of CD40 in immune surveillance is inevitably important. When engaged, CD40 enhances the ability of

antigen-presenting cells to stimulate T cells and facilitate their activation and maturation.<sup>50–52</sup> Robust activation of T cells through CD40 can promote adaptive immune responses against tumors and improve the survival probability.<sup>53,54</sup> Although we found a protective effect for CD40 through the Cox model after correcting the stage, KM estimates did not confirm the results. The protective effect of CD40 may be masked by other variables, whereas the negative correlation could be caused by unmeasured confounders or specific subgroups, highlighting the need for more research to clarify these findings.

Immune regulatory markers such as PDL1, TIM-3, B7-H3 and LAG3 play an integral role in the TME of NSCLC, influencing immune evasion and patient survival.<sup>55–57</sup> B7-H3 and regulatory T cells (Tregs) were discovered as potentially cooperating in tumor cell immune evasion and unfavorable outcomes.<sup>58</sup> B7-H3 has been shown to limit T cell proliferation, minimise cytokine production and suppress transcription factor activation.<sup>59–61</sup> Our finding replicates the negative impact of increased B7-H3 on patient survival. Multivariate analysis for the stroma confirms the unfavorable impact of LAG3, B7-H3 and PDL1, implying that when other covariates are controlled, the adverse effects of these markers become more pronounced. It has been shown that high GZMB is associated with the increased cytotoxic activity of tumor-infiltrating lymphocytes (TILs) and improved disease-free survival (DFS) and OS in multiple cancer types.<sup>62,63</sup> However, GZMB expression alone or coupled with markers like PD-L1 can variably affect both recurrence-free survival (RFS) and OS.<sup>62,64,65</sup> Our study supports these contradictory data by demonstrating that high GZMB expression is linked with poor survival. It implies that the impact of cytotoxic activity may vary depending on the cancer type and immunological context. CD14<sup>+</sup> cells in NSCLC contribute to the complexity of TME by increasing inflammation, which can potentially enhance tumor development and immune system evasion.<sup>66</sup> High CD14 expression is shown to be linked with a worse prognosis in lung squamous cell carcinoma (LUSC).<sup>67</sup> Schenk *et al.* also showed early-stage adenocarcinoma patients with increased CD14<sup>+</sup> cells experienced a lower median OS of 5.5 years compared to 10.7 years for those with moderate or low CD14 expression levels.<sup>68</sup> This negative effect is most likely caused by the role of myeloid-derived suppressor cells (MDSCs), in encouraging tumor spread and contributing to an immunosuppressive environment.<sup>69,70</sup> We also

confirmed that increased stromal CD14 is strongly related to poor survival outcomes corroborating the results of previous studies. CD66b's role in NSCLC includes immune landscape modulation like neutrophil extracellular trap (NET) development and contribution to tumor progression and metastasis.<sup>71,72</sup> We found an association between increased CD66b expression and shorter survival. One similar study found that elevated CD66b was related to an increased hazard ratio even after adjusting for other clinical covariates.<sup>73</sup> The same trend was seen in NSCLC patients treated with immune checkpoint inhibitors (ICI).<sup>74</sup>

We observed some discrepancies between CoxPH models and Kaplan–Meier results with a few potential reasons for this dominance, as follows. (1) Kaplan–Meier plots classify patients into groups according to cut-off points (e.g. median or quartiles), which may show significant group differences that would be less visible in a continuous analysis, such as CoxPH. (2) In accounting for numerous covariates, the CoxPH model may report less statistically significant results while Kaplan–Meier plots show the impact of a single marker on survival, especially when there are few confounding factors. (3) Kaplan–Meier plots might indicate early or late differences in survival rates that are not visible in the Cox model. If survival differences are concentrated at specific time intervals (e.g. early months or later years), they may appear as notable shifts in Kaplan–Meier curves, but are averaged out in CoxPH models.

## STUDY LIMITATIONS

Our study profiled two independently collected NSCLC tissue cohorts with single-core biopsies prepared in tissue microarray format. Tissue microarrays consist of limited tissue areas that are selected by pathologists to be representative of the tumor but may not account for the true tumor heterogeneity found across an entire full-face section. Furthermore, the post-surgery treatment information was not available for this study, preventing us from investigating their impact on the patient's survival.

## CONCLUSION

In this study, we analysed two NSCLC cohorts of over 100 patients before chemotherapy. We used Cox proportional hazards models and Kaplan–Meier estimates to assess patients' survival rates and discover protein markers affecting outcomes. Most

**Table 3.** Multiplex panel of antibodies.

Immune cell profiling panel				IO drug target panel			
Human protein core				Human protein module			
Beta-2-microglobulin	CD3	CD68	CTLA4	GZMB	PD1	4-1BB	LAG3
CD11c	CD4	CD8	Pan-cytokeratin	HLA-DR	PDL1	ARG1	OX40L
CD20	CD45	CD56	Fibronectin	Ki-67	SMA	B7-H3	STING
Ms IgG2a			Histone H3			GITR	TIM-3
Ms IgG1			S6			IDO1	VISTA
Rb IgG			GAPDH				

Immune activation status panel	Cell death panel	PI3K/AKT signalling panel	Immune cell typing panel	Pan-tumor panel
Human protein module	Human protein module	Human protein module	Human protein module	Human protein module
CD127	BAD	Pan-AKT	CD14	BCL-2
CD25	BCL6	MET	CD163	EpCAM
CD27	BCLXL	Phospho-AKT1(S473)	CD34	ER alpha
CD40	BIM	Phospho-GSK3B (S9)	CD45RO	HER2/ERBB2
CD80	CD95/Fas	Phospho-Tuberin (T1462)	CD66b	MART1
ICOS	GZMA	Phospho-GSK3A (S21)/ Phospho-GSK3B (S9)	FAP-alpha	NY-ESO-1
PD-L2	p53	INPP4B	FOXP3	PR
CD44	PARP	PLCG1		PTEN
	Cleaved Caspase 9	Phospho-PRAS40 (T246)		S100B
	Neurofibromin			

of the markers belong to the apoptosis, immune regulatory and immune response families. Furthermore, immune-modulating biomarkers, such as B7-H3 and PDL1, have significantly impacted immune evasion and tumor survival strategies. In addition, some cell adhesion molecules and myeloid cell markers have been associated with lowered survival rates. Taken together, this study provides an informed rationale for identifying biomarkers associated with OS in NSCLC. Further validation of findings is needed in orthogonal cohorts.

## METHODS

### Study design

This project has the Human Research Ethics Committee's approval and the University of Queensland's ratification. Two tissue microarrays (TMA) were constructed from resected lung specimens by Tristar Technologies Group (Washington, DC, USA). The clinical metadata included the NSCLC patients' age, stage at diagnoses and OS. TMAs contained 148 total single-patient cores, of which 102 were analysed in this study after excluding cores that failed tissue quality control or had no clinical follow-up data.

### Nanostring GeoMx DSP

Profiling of NSCLC TMAs was performed by Nanostring GeoMx DSP Technology as per manufacturer's instructions

(Seattle, Washington, USA). The samples were stained with anti-pan-cytokeratin (PanCK) and anti-CD45 morphology markers to visualise tumor (PanCK<sup>+</sup>) and non-tumor (PanCK<sup>-</sup>). A multiplex panel consisting of 78 antibodies for pan-tumor, immune activation, human immune cell, immune cell typing, immune-oncology (IO) drug target and cell death and PI3K/AKT were used per region of interest (ROI) on the slides (Table 3).

Through the ROI selection process, regions of interest were selected with a size of up to ~660 μm under the supervision of an anatomical pathologist. Segmentation of the ROI into two areas of interest (tumor and stroma) facilitated the targeted collection of oligos from specific locations.

Antibody barcodes were counted using the Nanostring nCounter<sup>®</sup> platform in accordance with the supplier's guidelines. External RNA Controls Consortium (ERCC) QC normalised data were exported from the instrument for bioinformatic analysis.

### Data analysis

Principal component analysis (PCA) was used to assess the data quality, and coefficients of variation were utilised to decide whether the RUV-seq normalising approach was appropriate (Figure 2a).<sup>75,76</sup> Differential analysis was performed by Limma.<sup>77</sup> Survival analysis by Kaplan–Meier was performed on median cut points of protein expression and the Cox proportional hazards model with continuous protein expression data. The CoxPH models for OS were developed using the CoxPH function in survival package in R (version 3.3–1). The survival object was created using Surv function in survival package. The *P*-values were

corrected using the false discovery rate for multiple correction method. The multivariate CoxPH model was also developed by incorporating the stage of disease information. To perform stepwise Cox regression with the specified parameters, the bidirectional selection method is employed, where the algorithm considers both forward addition and backward elimination steps. The significant levels selection criteria were applied to evaluate the significance of each variable to determine their inclusion or exclusion from the model. Additionally, the Breslow approximation method is used to handle ties in the data using StepReg package. HR values that were larger than 1 indicated an increased risk, whereas values that were less than 1 indicated a decreased risk.

## ACKNOWLEDGMENTS

This study was supported by Tour De Cure and Cancer Australia for AK. Open access publishing facilitated by Queensland University of Technology, as part of the Wiley - Queensland University of Technology agreement via the Council of Australian University Librarians.

## AUTHOR CONTRIBUTIONS

**Vahid Yaghoubi Naei:** Data curation; formal analysis; methodology; writing – original draft; writing – review and editing. **James Monkman:** Data curation; formal analysis; investigation; methodology; supervision; visualization; writing – review and editing. **Habib Sadeghirad:** methodology; writing – original draft; writing – review and editing. **Ahmed Mehdi:** Formal analysis; investigation; methodology; validation; visualization; writing – review and editing. **Tony Blick:** Formal analysis; investigation; methodology; writing – original draft; writing – review and editing. **William Mullally:** Methodology; writing – review and editing. **Ken O’Byrne:** Conceptualization; supervision; writing – review and editing. **Majid Ebrahimi Warkiani:** Conceptualization; funding acquisition; investigation; methodology; resources; supervision; writing – original draft; writing – review and editing. **Arutha Kulasinghe:** Conceptualization; funding acquisition; investigation; methodology; project administration; resources; supervision; writing – review and editing.

## CONFLICT OF INTEREST

The authors declare that they have no known competing financial interests or personal relationships that could have appeared to influence the work reported in this paper.

## DATA AVAILABILITY STATEMENT

The data supporting this study’s findings are available from the corresponding author upon reasonable request.

## REFERENCES

1. Siegel RL, Miller KD, Fuchs HE, Jemal A. Cancer statistics, 2021. *CA Cancer J Clin* 2021; **71**: 7–33.

2. Halliday PR, Blakely CM, Bivona TG. Emerging targeted therapies for the treatment of non-small cell lung cancer. *Curr Oncol Rep* 2019; **21**: 1–12.
3. Li Q, Yuan D, Ma C et al. A new hope: the immunotherapy in small cell lung cancer. *Neoplasma* 2016; **63**: 342–350.
4. García TC, Ruano-Ravina A, Candal-Pedreira C et al. Occupation as a risk factor of small cell lung cancer. *Sci Rep* 2023; **13**: 4727.
5. James BA, Williams JL, Nemesure B. A systematic review of genetic ancestry as a risk factor for incidence of non-small cell lung cancer in the US. *Front Genet* 2023; **14**: 1141058.
6. Alduais Y, Zhang H, Fan F, Chen J, Chen B. Non-small cell lung cancer (NSCLC): a review of risk factors, diagnosis, and treatment. *Medicine* 2023; **102**: e32899.
7. Parakh S, Leong TL, Best SA, Poh AR. Overcoming drug relapse and therapy resistance in NSCLC. *Front Oncol* 2023; **13**: 1230475.
8. Rolfo C, Caglevic C, Santarpia M et al. Immunotherapy in NSCLC: a promising and revolutionary weapon. *Immunotherapy* 2017; **995**: 97–125.
9. Lahiri A, Maji A, Potdar PD et al. Lung cancer immunotherapy: progress, pitfalls, and promises. *Mol Cancer* 2023; **22**: 40.
10. Hinshaw DC, Shevde LA. The tumor microenvironment innately modulates cancer progression. *Cancer Res* 2019; **79**: 4557–4566.
11. de Visser KE, Joyce JA. The evolving tumor microenvironment: from cancer initiation to metastatic outgrowth. *Cancer Cell* 2023; **41**: 374–403.
12. Quail DF, Joyce JA. Microenvironmental regulation of tumor progression and metastasis. *Nat Med* 2013; **19**: 1423–1437.
13. Wu T, Dai Y. Tumor microenvironment and therapeutic response. *Cancer Lett* 2017; **387**: 61–68.
14. Monkman J, Moradi A, Yunis J et al. Spatial insights into immunotherapy response in non-small cell lung cancer (NSCLC) by multiplexed tissue imaging. *J Transl Med* 2024; **22**: 239.
15. AlMusawi S, Ahmed M, Nateri AS. Understanding cell-cell communication and signaling in the colorectal cancer microenvironment. *Clin Transl Med* 2021; **11**: e308.
16. Monkman J, Kim H, Mayer A et al. Multi-omic and spatial dissection of immunotherapy response groups in non-small cell lung cancer. *Immunology* 2023; **169**: 487–502.
17. Jia Q, Wang A, Yuan Y, Zhu B, Long H. Heterogeneity of the tumor immune microenvironment and its clinical relevance. *Exp Hematol Oncol* 2022; **11**: 24.
18. Ge R, Wang Z, Cheng L. Tumor microenvironment heterogeneity an important mediator of prostate cancer progression and therapeutic resistance. *NPJ Precis Oncol* 2022; **6**: 31.
19. Sadeghi Rad H, Monkman J, Warkiani ME et al. Understanding the tumor microenvironment for effective immunotherapy. *Med Res Rev* 2021; **41**: 1474–1498.
20. Hsieh W-C, Budiarto BR, Wang Y-F et al. Spatial multi-omics analyses of the tumor immune microenvironment. *J Biomed Sci* 2022; **29**: 96.
21. Lewis SM, Asselin-Labat ML, Nguyen Q et al. Spatial omics and multiplexed imaging to explore cancer biology. *Nat Methods* 2021; **18**: 997–1012.

22. Monkman J, Taheri T, Ebrahimi Warkiani M et al. High-plex and high-throughput digital spatial profiling of non-small-cell lung cancer (NSCLC). *Cancers (Basel)* 2020; **12**: 3551.
23. Elhanani O, Ben-Uri R, Keren L. Spatial profiling technologies illuminate the tumor microenvironment. *Cancer Cell* 2023; **41**: 404–420.
24. Merritt CR, Ong GT, Church SE et al. Multiplex digital spatial profiling of proteins and RNA in fixed tissue. *Nat Biotechnol* 2020; **38**: 586–599.
25. Fitzmaurice C, Abate D, Abbasi N et al. Global, regional, and National Cancer Incidence, mortality, years of life lost, years lived with disability, and disability-adjusted life-years for 29 cancer groups, 1990 to 2017: a systematic analysis for the global burden of disease study. *JAMA Oncol* 2019; **5**: 1749–1768.
26. Li Y, Yan B, He S. Advances and challenges in the treatment of lung cancer. *Biomed Pharmacother* 2023; **169**: 115891.
27. Mamdani H, Matosevic S, Khalid AB, Durm G, Jalal SI. Immunotherapy in lung cancer: current landscape and future directions. *Front Immunol* 2022; **13**: 823618.
28. Hwang JK, Page BJ, Flynn D et al. Validation of the eighth edition TNM lung cancer staging system. *J Thorac Oncol* 2020; **15**: 649–654.
29. Pignon J-P, Tribodet H, Scagliotti GV et al. Lung adjuvant cisplatin evaluation: a pooled analysis by the LACE Collaborative Group. Database of Abstracts of Reviews of Effects (DARE): Quality-Assessed Reviews [Internet]: Centre for Reviews and Dissemination (UK). *J Clin Oncol* 2008; **26**: 3552–3559.
30. Insa A, Martín-Martorell P, Di Liello R et al. Which treatment after first line therapy in NSCLC patients without genetic alterations in the era of immunotherapy? *Crit Rev Oncol Hematol* 2022; **169**: 103538.
31. Zhang W, Ke Y, Liu X, Jin M, Huang G. Drug resistance in NSCLC is associated with tumor micro-environment. *Reprod Biol* 2022; **22**: 100680.
32. Kargl J, Zhu X, Zhang H et al. Neutrophil content predicts lymphocyte depletion and anti-PD1 treatment failure in NSCLC. *JCI Insight* 2019; **4**: e130850.
33. Patel SS, Rodig SJ. Overview of tissue imaging methods. *Methods Mol Biol* 2020; **2055**: 455–465.
34. Montero J, Haq R. Adapted to survive: targeting cancer cells with BH3 mimetics. *Cancer Discov* 2022; **12**: 1217–1232.
35. Adrain C, Martin SJ. The mitochondrial apoptosome: a killer unleashed by the cytochrome seas. *Trends Biochem Sci* 2001; **26**: 390–397.
36. Bratton SB, Salvesen GS. Regulation of the Apaf-1-caspase-9 apoptosome. *J Cell Sci* 2010; **123**: 3209–3214.
37. Goehe RW, Shultz JC, Murudkar C et al. hnRNP L regulates the tumorigenic capacity of lung cancer xenografts in mice via caspase-9 pre-mRNA processing. *J Clin Invest* 2010; **120**: 3923–3939.
38. Shultz JC, Goehe RW, Wijesinghe DS et al. Alternative splicing of caspase 9 is modulated by the phosphoinositide 3-kinase/Akt pathway via phosphorylation of SRp30a. *Cancer Res* 2010; **70**: 9185–9196.
39. Kim M, Vu NT, Wang X et al. Caspase 9b drives cellular transformation, lung inflammation, and lung tumorigenesis. *Mol Cancer Res* 2022; **20**: 1284–1294.
40. Sato C, Kitajima K. Polysialylation and disease. *Mol Asp Med* 2021; **79**: 100892.
41. Falconer RA, Errington RJ, Shnyder SD, Smith PJ, Patterson LH. Polysialyltransferase: a new target in metastatic cancer. *Curr Cancer Drug Targets* 2012; **12**: 925–939.
42. Moebius JM, Widera D, Schmitz J, Kaltschmidt C, Piechaczek C. Impact of polysialylated CD56 on natural killer cell cytotoxicity. *BMC Immunol* 2007; **8**: 13.
43. Jian Y, Zhang L, Gong L et al. CD56 polysialylation promotes the tumorigenesis and progression via the hedgehog and Wnt/ $\beta$ -catenin signaling pathways in clear cell renal cell carcinoma. *Cancer Cell Int* 2023; **23**: 319.
44. Sasca D, Szybinski J, Schüler A et al. NCAM1 (CD56) promotes leukemogenesis and confers drug resistance in AML. *Blood* 2019; **133**: 2305–2319.
45. Al-Shibli K, Al-Saad S, Donnem T, Persson M, Bremnes RM, Busund L-T. The prognostic value of intraepithelial and stromal innate immune system cells in non-small cell lung carcinoma. *Histopathology* 2009; **55**: 301–312.
46. Jin S, Deng Y, Hao J-W et al. NK cell phenotypic modulation in lung cancer environment. *PLoS One* 2014; **9**: e109976.
47. Zugazagoitia J, Gupta S, Liu Y et al. Biomarkers associated with beneficial PD-1 checkpoint blockade in non-small cell lung cancer (NSCLC) identified using high-plex digital spatial profiling. *Clin Cancer Res* 2020; **26**: 4360–4368.
48. Montesinos P, Rayón C, Vellenga E et al. Clinical significance of CD56 expression in patients with acute promyelocytic leukemia treated with all-trans retinoic acid and anthracycline-based regimens. *Blood* 2011; **117**: 1799–1805.
49. Georgakopoulou VE, Zygouris E, Damaskos C et al. Prognostic value of the immunohistochemistry markers CD56, TTF-1, synaptophysin, CEA, EMA and NSE in surgically resected lung carcinoid tumors. *Mol Clin Oncol* 2022; **16**: 31.
50. Soto M, Filbert EL, Yang H et al. Neoadjuvant CD40 agonism remodels the tumor immune microenvironment in locally advanced esophageal/gastroesophageal junction cancer. *Cancer Res Commun* 2024; **4**: 200–212.
51. Bullock TNJ. CD40 stimulation as a molecular adjuvant for cancer vaccines and other immunotherapies. *Cell Mol Immunol* 2022; **19**: 14–22.
52. Jian C-Z, Lin L, Hsu C-L et al. A potential novel cancer immunotherapy: agonistic anti-CD40 antibodies. *Drug Discov Today* 2024; **29**: 103893.
53. Beatty GL, Chiorean EG, Fishman MP et al. CD40 agonists alter tumor stroma and show efficacy against pancreatic carcinoma in mice and humans. *Science* 2011; **331**: 1612–1616.
54. Pang J, Liang B, Ding R, Yan Q, Chen R, Xu J. A denoised multi-omics integration framework for cancer subtype classification and survival prediction. *Brief Bioinform* 2023; **24**: bbad304.
55. D'Arrigo P, Tufano M, Rea A et al. Manipulation of the immune system for cancer defeat: a focus on the T cell inhibitory checkpoint molecules. *Curr Med Chem* 2020; **27**: 2402–2448.
56. Shimu AS, Wei H-x, Li Q, Zheng X, Li B. The new progress in cancer immunotherapy. *Clin Exp Med* 2023; **23**: 553–567.

57. Smith WM, Purvis IJ, Bomstad CN et al. Therapeutic targeting of immune checkpoints with small molecule inhibitors. *Am J Transl Res* 2019; **11**: 529–541.
58. Alberg AJ, Ford JG, Samet JM. Epidemiology of lung cancer: ACCP evidence-based clinical practice guidelines. *Chest* 2007; **132**: 295–555.
59. Prasad DV, Nguyen T, Li Z et al. Murine B7-H3 is a negative regulator of T cells. *J Immunol* 2004; **173**: 2500–2506.
60. Ling V, Wu PW, Spaulding V et al. Duplication of primate and rodent B7-H3 immunoglobulin V-and C-like domains: divergent history of functional redundancy and exon loss. *Genomics* 2003; **82**: 365–377.
61. Sun Y, Wang Y, Zhao J et al. B7-H3 and B7-H4 expression in non-small-cell lung cancer. *Lung Cancer* 2006; **53**: 143–151.
62. Mizoguchi K, Kawaji H, Kai M et al. Granzyme B expression in the tumor microenvironment as a prognostic biomarker for patients with triple-negative breast cancer. *Cancers (Basel)* 2023; **15**: 4456.
63. Chung JH, Ha JS, Choi J et al. Granzyme B for predicting the durable clinical benefit of anti-PD-1/PD-L1 immunotherapy in patients with non-small cell lung cancer. *Transl Cancer Res* 2022; **11**: 316–326.
64. Kinoshita F, Takada K, Wakasu S et al. Granzyme B (GZMB)-positive tumor-infiltrating lymphocytes in lung adenocarcinoma: significance as a prognostic factor and association with immunosuppressive proteins. *Ann Surg Oncol* 2023; **30**: 7579–7589.
65. Song X, Zhao G, Wang G, Gao H. Heterogeneity and differentiation trajectories of infiltrating CD8<sup>+</sup> T cells in lung adenocarcinoma. *Cancer* 2022; **14**: 5183.
66. Christofides A, Strauss L, Yeo A, Cao C, Charest A, Boussiotis VA. The complex role of tumor-infiltrating macrophages. *Nat Immunol* 2022; **23**: 1148–1156.
67. Li Z, Zhou B, Zhu X et al. Differentiation-related genes in tumor-associated macrophages as potential prognostic biomarkers in non-small cell lung cancer. *Front Immunol* 2023; **14**: 1123840.
68. Schenk EL, Boland JM, Withers SG, Bulur PA, Dietz AB. Tumor microenvironment CD14<sup>+</sup> cells correlate with poor overall survival in patients with early-stage lung adenocarcinoma. *Cancer* 2022; **14**: 4501.
69. Porrello A, Leslie PL, Harrison EB et al. Factor XIIIa—Expressing inflammatory monocytes promote lung squamous cancer through fibrin cross-linking. *Nat Commun* 2018; **9**: 1988.
70. Tian T, Gu X, Zhang B et al. Increased circulating CD14<sup>+</sup>HLA-DR<sup>-low</sup> myeloid-derived suppressor cells are associated with poor prognosis in patients with small-cell lung cancer. *Cancer Biomark* 2015; **15**: 425–432.
71. Zhang J, Jiang S, Li S et al. Nanotechnology: a new strategy for lung cancer treatment targeting pro-tumor neutrophils. *Engineering* 2023; **27**: 106–126.
72. Zhou J, Liu H, Jiang S, Wang W. Role of tumor-associated neutrophils in lung cancer. *Oncol Lett* 2023; **25**: 2.
73. Jain S, Ma K, Morris LGT. CD66b as a prognostic and predictive biomarker in patients with non-small cell lung cancer treated with checkpoint blockade immunotherapy. *Transl Cancer Res* 2023; **12**: 447–451.
74. Moutafi M, Martinez-Morilla S, Divakar P et al. Discovery of biomarkers of resistance to immune checkpoint blockade in NSCLC using high-plex digital spatial profiling. *J Thorac Oncol* 2022; **17**: 991–1001.
75. Molania R, Gagnon-Bartsch JA, Dobrovic A, Speed TP. A new normalization for Nanostring nCounter gene expression data. *Nucleic Acids Res* 2019; **47**: 6073–6083.
76. Risso D, Ngai J, Speed TP, Dudoit S. Normalization of RNA-seq data using factor analysis of control genes or samples. *Nat Biotechnol* 2014; **32**: 896–902.
77. Ritchie ME, Phipson B, Wu D et al. Limma powers differential expression analyses for RNA-sequencing and microarray studies. *Nucleic Acids Res* 2015; **43**: e47.

## Supporting Information

Additional supporting information may be found online in the Supporting Information section at the end of the article.



This is an open access article under the terms of the [Creative Commons Attribution-NonCommercial](#) License, which permits use, distribution and reproduction in any medium, provided the original work is properly cited and is not used for commercial purposes.